

Conformational disorder and energy migration in MEH-PPV with partially broken conjugation

M. M.-L. Grage

Department of Chemical Physics, Chemical Centre, Lund University, Box 124, S-22100 Lund, Sweden

P. W. Wood

School of Physics and Astronomy, University of St. Andrews, North Haugh, St. Andrews, Fife, KY16 9SS, United Kingdom

A. Ruseckas

Department of Chemical Physics, Chemical Centre, Lund University, Box 124, S-22100 Lund, Sweden and School of Physics and Astronomy, University of St. Andrews, North Haugh, St. Andrews, Fife, KY16 9SS, United Kingdom

T. Pullerits

Department of Chemical Physics, Chemical Centre, Lund University, Box 124, S-22100 Lund, Sweden

W. Mitchell and P. L. Burn

Dyson Perrins Laboratory, University of Oxford, South Parks Road, Oxford, OX7 3QY, United Kingdom

I. D. W. Samuel

School of Physics and Astronomy, University of St. Andrews, North Haugh, St. Andrews, Fife, KY16 9SS, United Kingdom

V. Sundström*

Department of Chemical Physics, Chemical Centre, Lund University, Box 124, S-22100 Lund, Sweden

(Received 5 September 2002; accepted 27 January 2003)

In order to obtain a better understanding of the role of conformational disorder in the photophysics of conjugated polymers the ultrafast transient absorption anisotropy of partially deconjugated MEH-PPV has been measured. These data have been compared to the corresponding kinetics of Monte Carlo-simulated polymer chains, and estimates of the energy hopping time and energy migration distances for the polymers have been obtained. We find that the energy migration in the investigated MEH-PPV is approximately 3 times faster than in previously studied polythiophenes. We attribute this to a more disordered chain conformation in MEH-PPV. © 2003 American Institute of Physics. [DOI: 10.1063/1.1562190]

INTRODUCTION

Organic conjugated polymers are a unique class of materials that combine the electronic properties of inorganic semiconductors with the flexible processing properties of plastics. They offer great potential for technological applications such as the next generation of flexible flat screen displays and tuneable laser sources.¹⁻⁶ In order for the technological applications to develop to their full potential it is essential to have a thorough understanding of the photophysics of these materials and the factors which affect it. The photophysics of the excited state is determined by the electronic structure of the polymer which is intimately linked to the conformation of the polymer. As conjugated polymers have tremendous scope for structural disorder, it is important to understand the conformation of a polymer in order to understand both the optical and electronic properties.

Several models have been proposed to describe the conformation of conjugated polymers. They broadly fall into two categories: (a) "wormlike" chains^{7,8} and (b) segmented chains.⁹⁻¹³ In the wormlike chain models the polymer is pic-

tured as having a small rotation between each repeat unit, leading to a smooth curving conformation. In the segmented chain models the chains are pictured as being made up of conjugated segments at large angles to each other. Here the flips in the chain represent the breaks in conjugation. In the wormlike chain the breaks in conjugation are less obvious: there is a slow loss of conjugation as one moves along the chain. Recent studies have suggested that MEH-PPV forms wormlike chains.^{14,15} However, it has been proposed¹⁶ that the presence of defects in the polymerization can have a dramatic effect on the chain conformation.

In this work we investigate how the extent of conjugation affects the conformation of the chain and electronic energy transfer within it. To achieve this we have used samples of partially deconjugated MEH-PPV where 34% of the vinylene linkages have been replaced by single bonds shown in Fig. 1. The connections between the electron delocalization and conformational disorder of our samples have been explored by probing the anisotropy of the ultrafast transient absorption. The observed decay in the anisotropy has been compared to the anisotropy calculated for Monte Carlo

*Author to whom correspondence should be addressed.

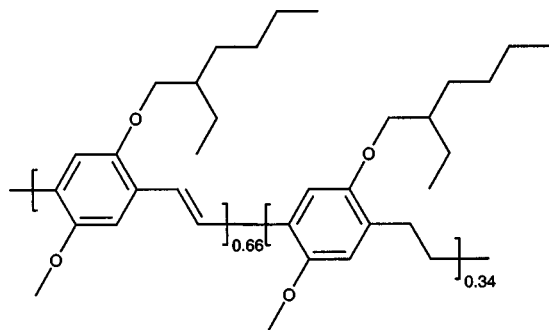


FIG. 1. Structure of the MEH-PPV polymer, with approximately 34% de-conjugation.

computer-generated polymer chains.¹⁷ The anisotropy of an excitation created by the absorption of linearly polarized light decays as the excitation is transferred from one segment to the next with differently oriented optical transition dipole moments. The transient anisotropy can thus be used to probe conformational disorder in the system. The simulations of the temporal behavior of the anisotropy will reveal the time scale of the transfer mechanism of the excitation and the energy migration distance along the polymer chain before trapping occurs. All our experiments are performed in dilute solution, and under these conditions only intrachain excitation transfer occurs and consequently interchain dynamics can be neglected. A polymer chain is generated by a partially correlated random walk with a hard sphere repulsion. The randomness—i.e., the angle between one segment and the next—is constrained by a Gaussian distribution. The width of this Gaussian is denoted as the disorder parameter and determines the disorder of the polymer. A large disorder parameter will give a wide distribution of angles between segments, which will result in a chain that contains more abrupt changes of direction. From a comparison between the calculated anisotropy of the simulated polymer chains and the experimental anisotropy we can fit (i) the disorder parameter, (ii) the time the excitation takes to transfer between segments (average pairwise hopping time), and (iii) the distance that the excitation travels along the chain before it is trapped (the migration length).

EXPERIMENT

In the partially conjugated MEH-PPV there were single bonds in place of 34% of the vinylene linkages. The synthesis of the partially conjugated MEH-PPV is described in detail elsewhere.¹⁸ All experiments were carried out in chlorobenzene solution, and care was taken to degass all samples immediately prior to performing the experiments (see Fig. 2). Measurements were repeated several times to ensure that they were consistent and that the samples had not degraded. As a further check against sample degradation, steady-state photoluminescence (PL) and absorption were compared before and after the experiment. The samples typically had a peak optical density of 0.1. Transient absorption kinetics were measured using a spectrometer based on an amplified Ti:sapphire laser system with a 5-kHz pulse repetition rate. Light pulses of ~ 80 fs full width at half maximum (FWHM)

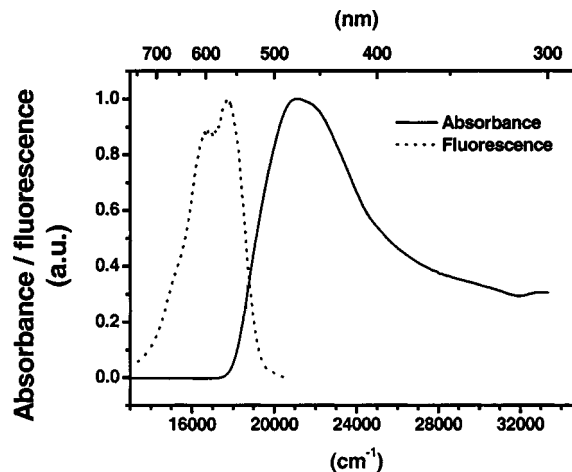


FIG. 2. Absorption and fluorescence spectra of the partially conjugated MEH-PPV in chlorobenzene.

from an optical parametric amplifier were used for excitation, and a white light continuum generated in a 5-mm-thick sapphire plate was used for the probe. The apparatus response function was approximately 120 fs. Signal and reference beams were spectrally filtered by a monochromator placed after the sample and detected using photodiodes. The anisotropy $r(t)$ was constructed as $r(t) = [\Delta A_{\parallel}(t) - \Delta A_m(t)] / 2\Delta A_m(t)$, where $\Delta A_{\parallel}(t)$ is the change in absorption with the pump and probe beams polarized parallel to each other and $\Delta A_m(t)$ is the change in absorption with the pump and probe beam polarizations at the magic angle (54.7°) to each other.

COMPUTER SIMULATIONS

The calculations consist of two stages: first the polymer conformations are generated, and then the anisotropy decays of these conformations are calculated. The polymer chains are constructed from MEH-PV monomers (Fig. 1) using a Monte Carlo method. In the calculations the excitation is assumed to be delocalized over several monomers which form a spectroscopic unit. Each monomer interacts with every other monomer of the polymer chain. The length of a spectroscopic unit is determined by the probability of having a break in conjugation; in our samples where 34% of the vinylene linkages have been replaced with single bonds, the spectroscopic units will on average be three monomers long. From size exclusion chromatography the chain lengths have been estimated to about 2000 monomers. However, since conjugated polymers are more rigid than the polystyrene standard used in GPC, the length of the chain is overestimated by this method.¹⁹ We have therefore in the calculations set the polymer chains to 300 spectroscopic units, leading to an average chain length of 900 monomers. When building the polymer chain, a vector assigned to each MEH-PV monomer defines the direction of it. The direction of the transition dipole moment is assumed to be the same, so the transition dipole moment is along the polymer chain. Assuming a harmonic bending potential,^{10,20} the direction vector of the neighboring monomer is selected from one of two Gaussian distributions:

$$P_i(\vec{r}_{n+1}) = \frac{1}{\sigma_i \sqrt{2\pi}} \exp\left(-\frac{(\vec{r}_{n+1} - \vec{r}_n)^2}{4\sigma_i^2}\right). \quad (1)$$

The first distribution [$P_1(\vec{r}_{n+1})$] is used to select the next direction vector 66% of the time and the second [$P_2(\vec{r}_{n+1})$] for the remaining 34%. The width of the first distribution (σ_1) determines the range of angles between monomers which are conjugated, and this is fixed to a low value, resulting in fairly straight conjugated parts. The width of the second distribution (σ_2) is the disorder parameter (which is a fitting parameter), and it is larger. It determines the range of angles between monomers where there is a break in conjugation (i.e., monomers which are linked by a single bond rather than vinylenic linkage). The polymer chain is not allowed to cross itself at any point on a chain, and the nearest distance that any two points may approach is set to 8 Å. This distance is given by the size of the side chains of the polymer and, together with the length of the monomer, has been estimated from the chemical structure.

The modeling of the energy transfer kinetics was performed assuming a hopping mechanism which previously has been used with success to model excitation transfer in polymers.^{17,21–27} The Förster transfer rate is calculated by summing the dipole–dipole interactions between each individual pair of monomers on different spectroscopic units. The orientation and position of the single monomer within a spectroscopic unit is thus needed, even though the excitation is assumed to be delocalized over a spectroscopic unit. The values resulting from this “line dipole” approximation are more realistic than the ones obtained from a raw point-dipole approximation for the spectroscopic unit as a whole. Calculating the Coulomb interaction between the corresponding transition densities²⁸ results in still more exact values of the Förster transfer rate, but needs much more effort.²⁹

In the following we use the method outlined by Pullerits and Freiberg,³⁰ which uses a Pauli master equation to describe the energy migration. In order to use the Pauli master equation the correlation time of the nuclear bath must be much shorter than the time scale of the site-to-site electronic jump process.³¹ Three-pulse stimulated photon echo peak shift experiments have revealed ~50 fs decay without recurrences,¹⁵ indicating that the bath correlation times are significantly shorter than the Förster hopping times used in the current work. Would the above separation of the time scales not be possible, one would have to apply master equation solutions with formally time-dependent transition rates^{32,33} or the rates which are dynamically correlated by excitation transfer and rotational Brownian motion.³⁴ Another example of an interfering mechanism would be intrasite structural relaxation.³⁵ These possibilities are not considered here since we do not see any indication of such processes in our experiments. However, in a recent similar study of polythiophene film, we observe a very fast initial depolarization that cannot be explained within the model of Förster hopping.³⁶

The Pauli master equation describes the energy migration

$$\frac{dp_j(t)}{dt} = \sum_i \left((1 - \delta_{ij})k_{ij} - \delta_{ik} \sum_k k_{ki} \right) p_i(t), \quad (2)$$

where $p_j(t)$ denotes the probability for the excitation being at spectroscopic unit j , δ_{ij} is the Kronecker delta function, and k_{ij} is the Förster rate for the excitation going from site i to site j [see Eq. (3) below]. The original Förster formula³⁷ and the formulas^{38,39} subsequently derived from it contain a number of parameters, including the Förster radius, natural lifetime, and refractive index. A number of these parameters may be empirically combined into the resonant hopping time τ_{hp} , the value of which can be estimated by comparison with experiment. Following this empirical approach we can write

$$k_{ij} = b_{ij} \frac{3}{2} \chi_{ij}^2 \frac{\theta_{ij}(\nu_{ij}) a^6}{\tau_{hp} r_{ij}^6}, \quad (3)$$

where

$$\chi_{ij} = \cos \alpha_{ij} - 3 \cos \beta_{ij} \cos \gamma_{ij}. \quad (4)$$

Here α_{ij} is the angle between the transition dipole moments of segments i and j ; β_{ij} and γ_{ij} are the angles between each dipole vector and the vector connecting them. r_{ij} is the distance between units i and j , and a is the distance between the centers of two coplanar monomers. $\theta_{ij}(\nu_{ij})$ is the spectral overlap between the donor luminescence and the acceptor absorption with energy difference $\nu_{ij} = \nu_j - \nu_i$ where ν_i and ν_j denote the energies of units i and j , respectively, and $\nu_{ij} = 0$ in the resonant case. $\theta_{ij}(\nu_{ij})$ is approximated by a Gaussian line shape. In order to satisfy the detailed balance equation in Eq. (4), we included a prefactor

$$b_{ij} = \begin{cases} 1 & \text{for } \nu_{ij} \geq 0, \\ b_{ij} = \exp(\nu_{ij}/kT) & \text{for } \nu_{ij} < 0, \end{cases} \quad (5)$$

so that one obtains

$$k_{ij} = b_{ij} \frac{3}{2} \frac{u}{\tau_{hp}} \theta_{ij}(\nu_{ij}) \sum_n \sum_m \frac{\kappa_{nm}^2}{r_{nm}^6}. \quad (6)$$

n and m run over the monomers of the donor and acceptor spectroscopic units, respectively, u is the length of a MEH-PV monomer, and the hopping time τ_{hp} is the Förster time for adjacent spectroscopic units connected in a straight line.

Since the experiments were carried out for excitation intensities well below excitation annihilation threshold, higher-order terms of the Pauli equation were omitted in our simulations. The parameters used in the program are Stokes' shift, homogeneous broadening, and inhomogeneous broadening, all estimated from steady-state spectra and the magic angle (isotropic) transient absorption decay. The hopping time (τ_{hp}) and the disorder parameter are obtained from the fitting procedure. The two parameters can be determined independently since the disorder parameter mainly affects the final (long-time) anisotropy and the hopping time determines the overall time scale of magic angle (isotropic) and anisotropy decays. The inhomogeneous broadening of the site energies was introduced via a Gaussian distribution of the transition energies of the spectroscopic units. The energy of a

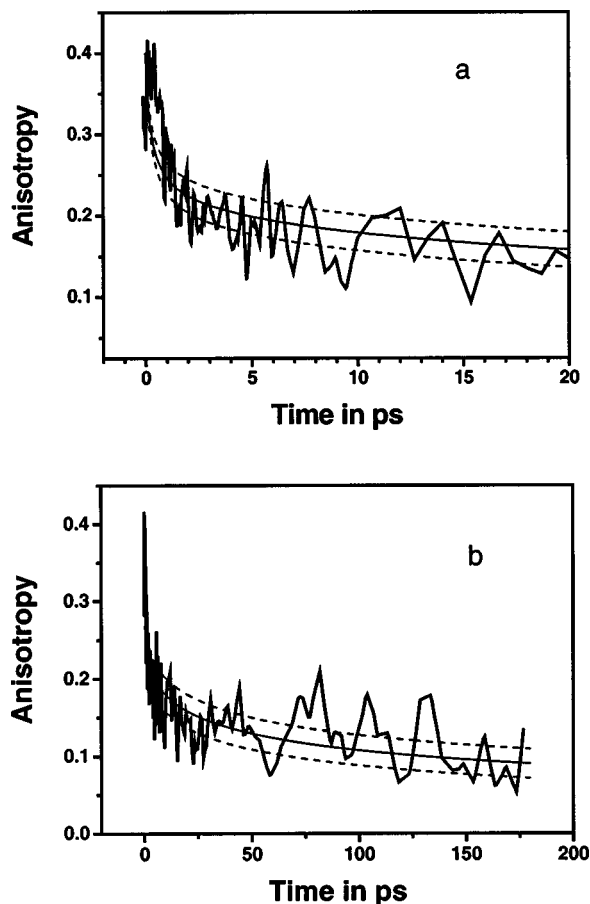


FIG. 3. Anisotropy decay of partially deconjugated MEH-PPV in chlorobenzene, on a short- (a) and a long- (b) time scale.

spectroscopic unit has also been correlated to its length using the energies given for MEH-PPV-like oligomers in chloroform reported by Meier *et al.*⁴⁰

RESULTS AND DISCUSSION

The measured transient anisotropy $r(t) = (\Delta A_{\parallel} - \Delta A_m) / (2\Delta A_m)$ is shown in Figs. 3(a) and 3(b). Initially, the anisotropy is 0.4, which is the theoretical value for a two-level system. In the first 20 ps it decays to 0.15 and then levels out at a somewhat lower value (~ 0.08) at long times. To gain information about the conformational disorder of the polymer chain simulations of the anisotropy decay as described above were carried out and compared to the experimental results. The simulated anisotropy [smooth curves, Figs. 3(a) and 3(b)] was obtained by averaging over 100 different realizations of the polymer chain, all constructed using the same disorder parameter. The different chain realizations were of somewhat varying lengths since the number of spectroscopic units was fixed to 300 and the lengths of the spectroscopic units were determined by the probability of a break in conjugation. In order to account for inhomogeneous broadening of site energies the anisotropy decay for each chain realization was averaged over 100 random sets of spectroscopic unit energies. These were taken from a Gaussian distribution of a width of 200 cm^{-1} centered on E_n (the energy of a spectroscopic unit with n monomer units). The

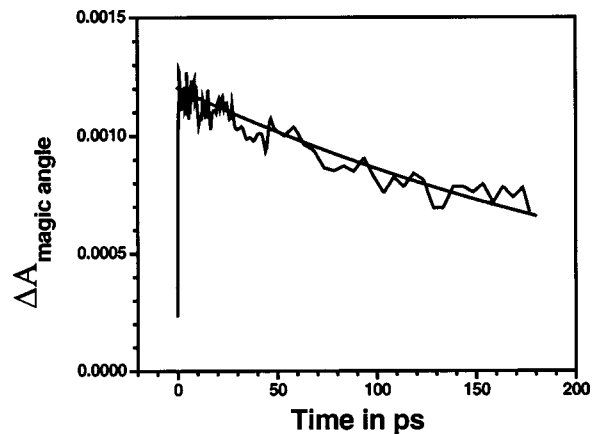


FIG. 4. Experimental and simulated magic angle decay.

average of the decays was taken as the anisotropy decay of this realization. The variation in the calculated anisotropy among the 100 different polymer chain realizations is shown by the dashed curves in Figs. 3(a) and 3(b). The long-time behavior of the decay [Fig. 3(b)] is governed by the overall conformational disorder, whereas the short-time behavior [Fig. 3(a)] involves the hopping time, homogeneous broadening, and inhomogeneous broadening. The homogeneous broadening of 2000 cm^{-1} was estimated from the width of the vibrational bands in the steady-state fluorescence spectrum (Fig. 2). The simulations of the anisotropy resulted in an average pairwise hopping time of 0.3 ps between adjacent spectroscopic units and an excitation travel distance of 7 ± 3 spectroscopic units, showing that excitations visit only a small fraction of the polymer chain. The magic angle (isotropic) decay was also simulated, and it turned out that this decay just reflected the time constant of the dissipation from the system (Fig. 4).

In Fig. 5 three anisotropy decay curves contributing to the average in Fig. 3 are shown and the polymer chains giving rise to these calculated anisotropies are shown in Fig. 6. All configurations are generated using the same disorder parameter. The simulated anisotropy decays for the three different realisations of the polymer are very similar, but a few distinctions can still be made. Both the average pairwise

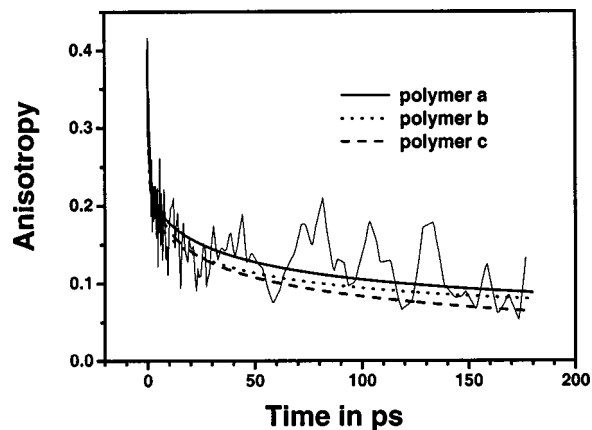


FIG. 5. Anisotropy of three different realizations together with the experimental anisotropy.

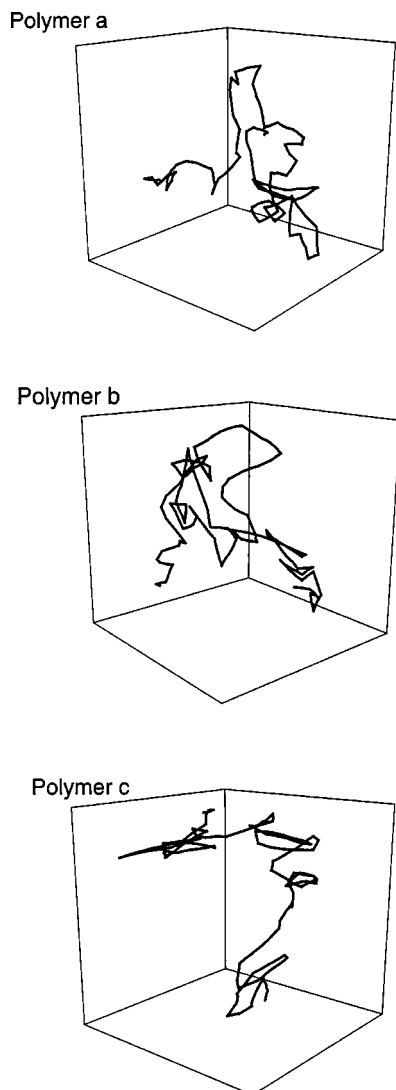


FIG. 6. Three different realizations of polymer chains giving rise to the anisotropy curves in Fig. 5.

hopping times and the mean excitation transfer distances vary for the three different realizations. Polymer **a** consists of one spectroscopic unit of 11 monomers, 2 spectroscopic units of 9 monomers, and the rest are very short. The mean excitation transfer distance is 6 spectroscopic units, and the pairwise hopping time is 0.4 ps. The longest spectroscopic units of polymer **b** are 6 monomers long, leading to a somewhat shorter average pairwise hopping time of 0.3 ps and an excitation transfer distance of 8 spectroscopic units. Polymer **c** has the longest excitation transfer distance of the three, 13 spectroscopic units, the shortest average pairwise hopping time, 0.2 ps, and the longest spectroscopic unit is 5 monomers long. It can be concluded that the differences for the anisotropy decays, hopping times, and mean excitation transfer distances mainly arise as a consequence of the microscopic variations of the different realizations.

The long-time level of the anisotropy decay monitors the relative orientations of the segments where the excitation is created and trapped. This relative orientation will depend on the conformational disorder of the polymer and how far along the chain the excitation travels before it is trapped. The

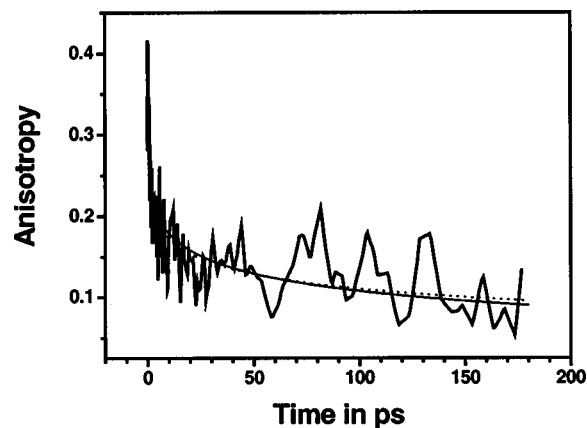


FIG. 7. Anisotropy decays from experiment and the two simulations: the energy-length correlated (solid line) and random (dotted line).

distance that the excitation travels will be determined by the spectral inhomogeneity of the polymer, which is determined by the breaks in conjugation. In a polymer with a small spectral inhomogeneity an excitation will be able to travel farther than in a polymer with large inhomogeneity. For polymers with a similar level of disorder, but different spectral inhomogeneities, the long-time anisotropy value will be different. This explains the differences in the long-time anisotropies of polymers **a**, **b**, and **c**. The long segment of 11 monomers of polymer **a** is contributing to the higher level of the long-time anisotropy as its low energy will act as a trap for the excitation. The relatively long sections having a straight conformation in this realization contribute further to the high long-time level of the anisotropy. Polymer **c**, on the other hand, contains very few red segments, and the energy has the possibility to transfer very efficiently along the chain, as is reflected by the long mean travel distance.

In addition to simulations where the energy of a segment is correlated to its length, simulations were also performed using a random distribution independent of segment length. In Fig. 7 the anisotropy decays from experiment and the two simulations are shown. The anisotropy curves calculated with the two different methods of assigning the energy of a segment are very similar. Both methods result in a mean travel distance of 7 spectroscopic units and a pairwise hopping time of 0.3 ps for 34% deconjugated MEH-PPV. These results show that the calculated energy transfer dynamics are not very sensitive to the details of the site energy assignment.

A polymer with fewer conjugation breaks is expected to be stiffer, have less conformational disorder, and should therefore be characterized by higher anisotropy. A simulation shown in Fig. 8 for an MEH-PPV polymer chain with 10% deconjugation, but all other parameters the same as the polymers in Fig. 6, verified this expectation. The calculated anisotropy decay of the chain with fewer conjugation breaks levels out at higher long-time value of the anisotropy. The decay of anisotropy from the initial value of 0.4 to the constant level is also slower than in the 34% deconjugated chain and has an average pairwise hopping time of approximately 1 ps. This is a result of the much longer average segment length (10 monomers) of the 10% deconjugated chain, which includes more red segments with slower hopping times (see

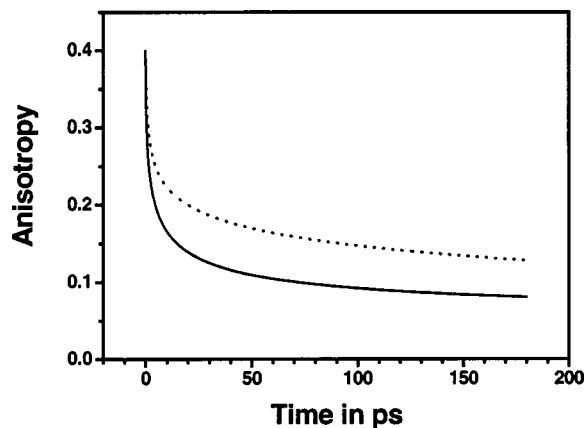


FIG. 8. Simulated anisotropy decays with 34% (solid line) and 10% (dotted line) broken conjugation.

also description of the results in Fig. 5). Preliminary measurements of fully conjugated MEH-PPV in solution displaying high long-time anisotropies ($r > 0.2$, not shown) support this conclusion.

A recent study on a polythiophene with bulky side chains¹⁷ suggests that the polythiophene has a flexible chain with conjugation lengths of 6 to 8 monomers⁴¹ (corresponding to 24–32 Å) and a slower (~ 1 ps) hopping time than the deconjugated MEH-PPV studied here. We assign this difference to the fact that the partially deconjugated MEH-PPV has many short spectroscopic units (2–3 monomers corresponding to 28–42 Å) as well as a large conformational disorder, on which the hopping will be very efficient due to short distances and good spectral overlap. The disorder we found for polythiophene is much smaller, resulting in a wormlike conformational structure, leading to a more linear arrangement of the spectroscopic units which results in a longer excitation transfer distance for a single hop. To break the conjugation in polythiophene one has to introduce an extra single bond between the thiophene monomers or deform the ring (see Fig. 9), while according to quantum chemical calculations²⁹ rotating a thiophene monomer around the single-linkage bond will only result in a weakening of the conjugation. The difference may have a consequence for how well the hopping model describes the motion of the excitation along the polymer chain for the two different polymers. In the case of partially conjugated MEH-PPV the hopping model is expected to describe the motion of the excitation quite well since the spectroscopic units are separate entities linked by single bonds. In polythiophene the

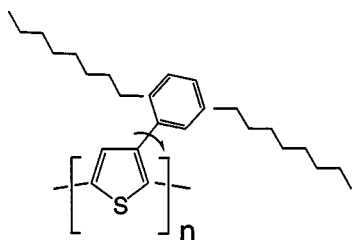


FIG. 9. Structure of poly(3-(2,5-dioctylphenyl)thiophene).

motion may very well be partly coherent, and the hopping model is then an approximation.

SUMMARY

The degree of electron delocalization in conjugated polymers is intimately linked to the conformation of the polymer. We have investigated the effect of reducing the electron delocalization in MEH-PPV by replacing 34% of the vinylene linkage double bonds with single bonds on the conformation of, and the energy transfer within, the polymer chain. The conformation and excitation transfer were probed by measuring the transient anisotropy of our samples in dilute solution and comparing the results to the calculated anisotropy decay of Monte Carlo computer-generated polymer chains. The excitation transfer along the polymer chains was simulated using a Pauli master equation based on a Förster incoherent hopping mechanism. Using our simulations, we have calculated the possible conformations of the polymer chains, the average pairwise hopping time between adjacent spectroscopic units within the chain, and distance the excitation travels before it is trapped.

ACKNOWLEDGMENTS

This collaboration was supported by the TMR program “Access to Large Scale Facilities,” Contract No. HPRI-CT-1999-00041. Financial support from the Swedish Natural Science Research Council (NFR), the Knut and Alice Wallenberg Foundation, and the Trygger Foundation is also gratefully acknowledged.

- O. Inganäs, M. Bergren, M. R. Andersson, G. Gustafsson, T. Hjertberg, O. Wennerström, P. Dyreklev, and M. Granström, *Synth. Met.* **71**, 2121 (1995).
- G. Gustafsson, Y. Cao, G. M. Treacy, F. Klavetter, N. Colaneri, and A. J. Heeger, *Nature (London)* **357**, 477 (1992).
- J. H. Burroughes, D. D. C. Bradley, A. R. Brown, and A. B. Holmes, *Nature (London)* **347**, 539 (1990).
- M. R. Andersson, M. Bergren, G. Gustafsson, T. Hjertberg, O. Inganäs, and O. Wennerström, *Synth. Met.* **71**, 2183 (1995).
- H. Sirringhaus, N. Tessler, and R. H. Friend, *Science* **280**, 1741 (1998).
- I. D. W. Samuel, *Philos. Trans. R. Soc. London, Ser. A* **358**, 193 (2000).
- K. S. Schweizer, *J. Chem. Phys.* **85**, 4181 (1986).
- Z. G. Soos and K. S. Schweizer, *Chem. Phys. Lett.* **139**, 196 (1987).
- G. Rossi, R. R. Chance, and R. Silbey, *J. Chem. Phys.* **90**, 7594 (1989).
- S. N. Yaliraki and R. Silbey, *J. Chem. Phys.* **103**, 6248 (1995).
- B. E. Kohler and I. D. W. Samuel, *J. Chem. Phys.* **103**, 6248 (1995).
- B. E. Kohler and J. C. Woehl, *J. Chem. Phys.* **103**, 6253 (1995).
- K. S. Schweizer, *J. Chem. Phys.* **85**, 4181 (1986).
- R. Chang, J. H. Hsu, W. S. Fann *et al.*, *Chem. Phys. Lett.* **317**, 142 (2000).
- G. D. Scholes, D. S. Larsen, G. R. Fleming, G. Rumbles, and P. L. Burn, *Phys. Rev. B* **61**, 13 670 (2000).
- D. Hu, J. Yu, K. Wong, B. Bagchi, P. J. Rossky, and P. F. Barbara, *Nature (London)* **405**, 1030 (2000).
- M. M.-L. Grage, T. Pullerits, A. Ruseckas, M. Theander, O. Inganäs, and V. Sundström, *Chem. Phys. Lett.* **339**, 96 (2001).
- G. R. Webster, S. A. Whitelegg, D. D. C. Bradley, and P. L. Burn, *Synth. Met.* **119**, 269 (2001).
- I. Ledoux, I. D. W. Samuel, J. Zyss, S. N. Yaliraki, F. J. Schattenmann, R. R. Schrock, and R. J. Silbey, *Chem. Phys.* **245**, 1 (1999).
- H. Kleinert, *Path Integrals in Quantum Mechanics, Statistics and Polymer Physics* (World Scientific, Singapore, 1990), p. 590.
- A. D. Stein, K. A. Peterson, and M. D. Fayer, *Chem. Phys. Lett.* **161**, 16 (1989).
- J. D. Byers, W. S. Parsons, R. A. Friesner, and S. E. Webber, *Macromolecules* **23**, 4835 (1990).

- ²³J. D. Byers, W. S. Parsons, and S. E. Webber, *Macromolecules* **25**, 5935 (1990).
- ²⁴B. Mollay, U. Lemmer, R. Kersting, R. F. Mahrt, H. Kurz, H. F. Kauffmann, and H. Bässler, *Phys. Rev. B* **50**, 10769 (1994).
- ²⁵M. Schiedler, U. Lemmer, R. Kersting *et al.*, *Phys. Rev. B* **54**, 5536 (1996).
- ²⁶R. Kersting, B. Mollay, M. Rusch, J. Wenisch, G. Leisning, and H. F. Kauffmann, *J. Chem. Phys.* **106**, 2850 (1997).
- ²⁷K. Brunner, A. Tortschanoff, Ch. Warmuth, H. Bässler, and H. F. Kauffmann, *J. Phys. Chem. B* **104**, 3781 (2000).
- ²⁸B. P. Krueger, G. D. Scholes, and G. R. Fleming, *J. Phys. Chem. B* **102**, 5378 (1997).
- ²⁹W. J. D. Beenken (private communication).
- ³⁰T. Pullerits and A. Freiberg, *Biophys. J.* **63**, 879 (1992).
- ³¹C. R. Gouchanour, C. R. Andersen, and M. D. Fayer, *J. Chem. Phys.* **70**, 4254 (1979).
- ³²A. K. Harrison and R. Zwanzig, *Phys. Rev. A* **32**, 1072 (1985).
- ³³S. D. Druger, M. A. Ratner, and A. Nitzan, *Phys. Rev. B* **31**, 3939 (1985).
- ³⁴G. H. Fredrickson, *J. Chem. Phys.* **88**, 5291 (1988).
- ³⁵L. J. Rothberg, M. Yan, F. Papadimitrakopoulos, M. E. Galvin, W. E. Kwock, and M. E. Miller, *Synth. Met.* **80**, 41 (1996).
- ³⁶M. M.-L. Grage, Y. Zaushitsyn, A. Yartsev, M. Chachisvilis, V. Sundström, and T. Pullerits, *Phys. Rev. B* (to be published).
- ³⁷T. Förster, *Ann. Phys. (N.Y.)* **6**, 55 (1948); in *Modern Quantum Chemistry*, edited by O. Sinanoglu (Academic, New York, 1953), Vol. III.
- ³⁸J. M. Jean, G. R. Fleming, and T. G. Owens, *Biophys. J.* **56**, 1203 (1989).
- ³⁹T. Pullerits and A. Freiberg, *Chem. Phys.* **149**, 409 (1990).
- ⁴⁰M. Meier, U. Stalmach, and H. Kolshorn, *Acta Polym.* **48**, 379 (1997).
- ⁴¹R. A. J. Janssen, L. Smilowitz, N. S. Saricifti, and D. Moses, *J. Chem. Phys.* **101**, 1787 (1994).